JOURNAL OF MATERIALS SCIENCE 32 (1997) 1765–1773

Dynamics of directional coarsening in binary alloys: Monte-Carlo simulation

JUN-MING LIU
National Laboratory of Solid State Microstructures, Nanjing University, Nanjing 210093, and Center for Advanced Studies in Science and Technology of Microstructures, Nanjing 210093, People's Republic of China

Directional coarsening in binary alloys during phase separation has been simulated by means of the Monte-Carlo technique based on the spin-exchange Ising model in two-dimensional squared lattices. A uniaxial interaction has been imposed on the Hamiltonian of the standard Ising system in order to achieve directional coarsening of the domained structure. Characterization of the domained structure with the snapshot patterns, the spatial correlation function and the structure function, is also given. It has been found that with time this system exhibits highly uniaxially anisotropic patterns of the domain morphology and the correlation function, and also achieves a uniaxially textured structure function. Under such a uniaxially anisotropic interaction, the dynamics of the system still achieves a good agreement with the dynamic scaling hypothesis. Towards the later stage, the kinetics of coarsening acquires a growth exponent of 1/3, the same as the well-known value in the isotropic alloys.

1. Introduction

When a binary solid alloy is submitted into the immiscible gap of the phase diagram, phase separation proceeds inside the alloy via either the nucleation-and-growth mechanism or spinodal decomposition, depending on instability of the alloy. This process has been of interest for decades, not only from the point of view of technological applications, but also as a representative example of first-order phase transitions [1–6]. For a comprehensive review of several aspects of this extensive field, readers are referred to the recent review articles [2, 3]. Here, remarks are confined to the morphology of domains and the general dynamics of phase separation in alloys. In a system which exhibits isotropic property of structures, the morphology of domains shows no considerable anisotropy and the dynamics of phase separation can be quite well described by the dynamic scaling hypothesis [7–10], with the kinetic exponent of coarsening being 1/3, as predicted by the Lifshitz–Slyozov–Wagner theory [11–16]. The experimental verifications of this theory have always been made in those alloys which are microstructurally isotropic, such as structural glasses, liquid mixtures and also some metallic alloys [2, 7, 17, 18]. Nevertheless, systematic demonstration of the dynamic scaling concept has been presented in the mode system by using computer simulations [16], preferably by the Monte-Carlo technique [19,20]. The standard Ising model with a conserved-order parameter, where the chemical potentials between the like-pair and unlike-pair of species are the driving force, and the configuration entropy is the resisting force to the chemical potential, takes part in modulating the structure has been applied in the simulations and represents one of the typical mode systems. As only the nearest-neighbouring interaction of a species-pair is involved, the isotropic morphology of domains will be observed. The dynamic scaling hypothesis in these systems has been widely approved.

However, in real alloy systems, the morphology of domains during phase separation is considerably influenced by many factors, such as the anisotropy of interfacial energy and the internal elastic energy arising during phase separation, due to the difference in atomic size of the two species or the lattice symmetry or the externally imposed load as well [21–25]. Generally speaking, growth of domains in such a system prefers orientations with minimum energy (interfacial energy, elastic softening, etc.). This is the so-called "directional coarsening" [26]. For the case of low alloy composition, where isolated second phases are formed, plate-like or rod-like patterns are observed in elastically anisotropic cubic matrices, whereas an anisotropic modulating structure will form as the alloy composition is high, in order to minimize the coherency strain energy [2]. On the other hand, under a uniaxial external load, the directional coarsening phenomenon will be observed in alloys, where the precipitates exhibit a morphology consisting of either plate-like structures perpendicular to, or rod-like structures parallel to, the stress direction [27–29]. This phenomenon has been studied macroscopically by continuum models [23]and simulated microscopically by the Monte-Carlo (MC) method [26, 30, 31],

0022–2461

revealing varied morphologies of domains and mechanical properties in some relatively simple mode systems.

Nevertheless, to the author's knowledge, a systematic study of the dynamics of phase separation in such a system which exhibits directional coarsening of domains, has still not been carried out. In particular, the dynamic scaling behaviour in this system has not been checked. Experimentally, the currently applied small-angle scattering (X-ray, neutron) techniques meet difficulty in evaluating anisotropic dynamic data of phase separation in the structurally anisotropic systems, in order to question the validity of the dynamic scaling concept. Instead, the Monte-Carlo simulation based on a mode system would be a powerful tool for such a purpose. This paper reports a study of this problem by means of the Monte-Carlo technique. A simple thermodynamic model is proposed and the study was confined to the domain morphology and dynamic scaling of phase separation in alloys with uniaxially anisotropic interaction, where the directional coarsening proceeds. Microscopically, this interaction may be imposed by either an external field (load) or an anisotropic potential between species. The dynamic characteristics of directional coarsening in such a system are shown and the dynamic scaling approach is demonstrated.

2. Model and simulation procedure

As we are concerned mainly with the dynamics of directional coarsening, we apply an Ising system which is simple but general. Starting from a two-dimensional squared lattice of size $L \times L$ with periodic boundary conditions, we consider a binary system AB with each site of the lattice occupied by either species A or B. The alloy composition is $C_0 = N_B/(N_A + N_B)$, where N_A and N_B are the numbers of A- and B-type species in the lattice. The order parameter for the present system is the local alloy composition and it is conserved. Because only the chemical potential between two nearest-neighbouring species is considered and denoted by $J(>0)$, we can write the Hamiltonian of this mode system as

$$H = -J \sum_{\langle i,\, j\rangle} S_i S_j \tag{1}$$

where $\langle i, j\rangle$ represents summation over all lattice sites and $S_i = 1$ if site i is occupied with species A, otherwise $S_i = -1$. Clearly, as $i = \langle m, n\rangle$, we have $j = \langle m-1, n\rangle$, $\langle m+1, n\rangle$, $\langle m, n-1\rangle$ and $\langle m, n+1\rangle$.

When dealing with a uniaxially anisotropic interaction to be imposed to the system defined by Equation 1, the simplest case is to add a competitive term which is applied only along one axis of the lattice. Here we choose the Y-axis. Then Equation 1 can be rewritten as

$$H = -J \sum_{\langle i,\, j\rangle} S_i S_j + \sigma \sum_{\langle i,\, j\rangle}^{y-y} S_i S_j \tag{2}$$

where σ is a positive constant which scales the uniaxially anisotropic interaction, $y - y$ indicates that the summation is done only along the Y-axis. $\sigma > 0$ indicates the imposition along the Y-axis of a uniaxially anisotropic interaction which is opposite to the species-pair interaction scaled by J. This corresponds to, for example, a stretching load imposed on the system along the Y-axis. As $\sigma > 0$, the directional coarsening is expected to proceed along the X-axis, otherwise, it will proceed along the Y-axis. As $i = \langle m, n\rangle$, we have $j = \langle m, n-1\rangle$ and $\langle m, n+1\rangle$. With respect to the elastic energy arising during phase separation, one parameter σ, may not be enough to characterize the effect. However, as the first-order approximation, it makes sense, because it has been revealed that under an external load, the elastic energy inside both phase-separating phases has a uniform distribution, giving no considerable effect on the species-pair interaction along the X-axis [26].

In such a simple system defined by Equation 2, directional coarsening can proceed as suitable values of J and σ are given. The conventional spin-exchange Ising model is applied to simulate the phase separation. We propose below a simulation procedure which is similar to the Kawasaki mode. For given system parameters C_0, J and σ, and an initial lattice configuration where species A and B are imposed in random, we calculate by Equation 2 the interaction energy of a species at each site i with its four nearest neighbours. A random number, R_1, is generated, and if R_1 falls into the ith interval, the species at site i is chosen to exchange with one of its four nearest neighbours in the next step. The exchanging probability $P_{i\leftrightarrow j}$ between two species at site i and one of its four neighbours, j, is [31]

$$P_{i\leftrightarrow j} = \exp(-\Delta E_{i\leftrightarrow j}/k_B T) \Big/ \sum_{j=1}^{5} \exp(-\Delta E_{i\leftrightarrow j}/k_B T) \tag{3}$$

where $\Delta E_{i\leftrightarrow j}$ represents the difference in the energy over all the lattice before and after the $i\leftrightarrow j$ exchange, k_B is the Boltzmann constant and T is temperature. Here, as $i = \langle m, n\rangle$, we have $j = \langle m, n\rangle$, $\langle m-1, n\rangle$, $\langle m+1, n\rangle$, $\langle m, n-1\rangle$ and $\langle m, n+1\rangle$, respectively. Then, another random number, R_2, is generated and an exchanging operation between species at sites i and j is handled. This process is repeated until a given number of species exchanges is reached. We apply the unit mcs to scale the time for phase separation. One mcs represents completed $L \times L$ species exchanges.

With respect to a highly anisotropic structure consisting of two phases, some vectored dynamic quantities must be defined in order to characterize the dynamics of phase separation. We define the spatial correlation function $g(x, y, t)$ and structure function $S(k_x, k_y, t)$ of the lattice at time t

$$g(x, y, t) = \frac{1}{L \times L} \sum_{m,n}^{L\times L} (G(m, n, t) - C_0) \times (G(m + x, n + y, t) - C_0) \tag{4a}$$

$$S(k_x, k_y, t) = \frac{1}{L \times L} \sum_{x,y}^{L\times L} g(x, y, t) \exp(-i\boldsymbol{k}\boldsymbol{r}) \tag{4b}$$

$$\boldsymbol{k} = \boldsymbol{i}k_x + \boldsymbol{j}k_y, \quad \boldsymbol{r} = \boldsymbol{i}x + \boldsymbol{j}y \tag{4c}$$

where $G(m, n, t) = 0$ if site (m, n) is occupied by species A, otherwise $G(m, n, t) = 1$; x and y, k_x and k_y are the coordinates and wave-vectors along X-axis and Y-axis, respectively. From Equation 4, we can also define the axially oriented and radially averaged correlation functions and structure functions

$$g(x) = g(x, 0, t) \tag{5a}$$

$$g(y) = g(0, y, t) \tag{5b}$$

$$g(r) = \frac{1}{M} \sum_{|r| \le r < |r|+1} g(x, y, t) \tag{5c}$$

$$\boldsymbol{r} = \boldsymbol{i}x + \boldsymbol{j}y \tag{5d}$$

$$S(k_x) = S(k_x, 0, t) \tag{5e}$$

$$S(k_y) = S(0, k_y, t) \tag{5f}$$

$$S(k_r) = \frac{1}{N} \sum_{|k| \le k_r < |k|+1} S(k_x, k_y, t) \tag{5g}$$

$$\boldsymbol{k} = \boldsymbol{i}k_x + \boldsymbol{j}k_y \tag{5h}$$

where M is the number of discretized $g(x, y, t)$ which satisfies $|r| \le r < |r| + 1$ and N is the number of discretized $S(k_x, k_y, t)$ which fall into range $[|k|, |k| + 1)$, over all the lattice sites. $g(r)$ and $S(k_r)$ represent a radial average of $g(x, y, t)$ and $S(k_x, k_y, t)$, respectively.

In this paper, we will report our simulated results on systems of $C_0 = 0.30$, $J = 0.60k_BT$ and $\sigma = 0.50k_BT$, and $C_0 = 0.50$, $J = 0.60k_BT$ and $\sigma = 0.50k_BT$. The former system exhibits isolated second phases during phase separation and the latter shows inter-connected domain structure. As a comparison, we have also simulated phase separation in two systems of no uniaxially anisotropic interaction, i.e. of $C_0 = 0.30$, $J = 0.60k_BT$ and $\sigma = 0$, and $C_0 = 0.50$, $J = 0.60k_BT$ and $\sigma = 0$. For each of these systems, four repeated simulations starting from different seeds for random number generator, have been made and the averages of quantities over the four simulations are presented below.

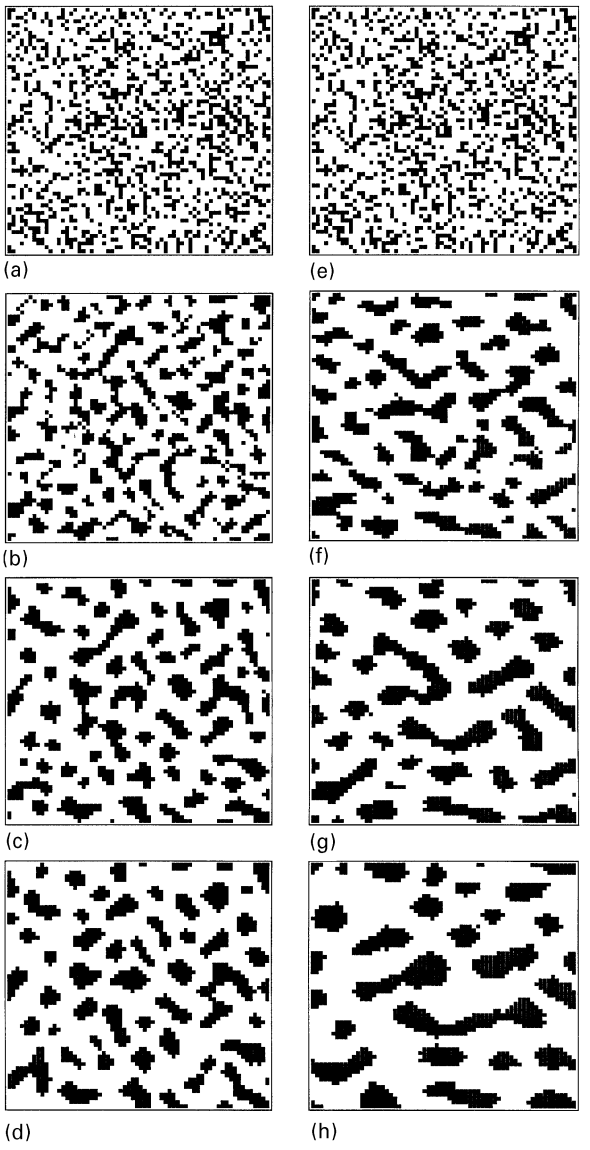

Figure 1 The snapshot pictures of the domained structure at several times for the systems (a–d) $C_0 = 0.30$, $J = 0.60k_BT$ and $\sigma = 0$ and (e–h) $C_0 = 0.30$, $J = 0.60k_BT$ and $\sigma = 0.50k_BT$. The solid spots are for B-type species and the open spaces for A-type species. The time scales are: (a) $t = 0$, (b) $t = 10$ mcs, (c) $t = 900$ mcs, (d) $t = 3400$ mcs, (e) $t = 0$, (f) $t = 100$ mcs, (g) $t = 1000$ mcs, (h) $t = 3400$ mcs.

3. Simulated results and discussion

3.1. Morphology of domains

Fig. 1 presents the snapshot pictures at several times for (a–d) a system of $C_0 = 0.30$, $J = 0.60k_BT$ and $\sigma = 0$ (isotropic case), and (e–h) a system of $C_0 = 0.30$, $J = 0.60k_BT$ and $\sigma = 0.50k_BT$ (uniaxially anisotropic case). The time scales are given in the caption. The solid spots are for B-type species and the empty spaces are for A-type species. Clearly, for the case of isotropic interaction ($\sigma = 0$), phase separation proceeds via growth and coarsening of isotropic and isolated second-phase domains. Splitting into two small equiaxed domains of a large rod-like domain is frequently observed during phase separation. The growth of larger domains is compensated by shrinkage of smaller domains. However, for the case of $\sigma = 0.50k_BT$, even at the early stage, most domains, as shown, exhibit rod-like morphology along the X-axis. The directional coarsening has been clearly revealed. With the other characteristics of the morphological evolution remaining similar to the case of $\sigma = 0$, the coarsening kinetics are shown to be much faster than the case of $\sigma = 0$, characterized by coarser domains and larger domain spacing. This is quite interesting because compared to the system of $\sigma = 0$, the system of $\sigma = 0.50k_BT$ has a lower average binding energy for each species and it should acquire a finer microstructure. Nevertheless, owing to the conserved-order parameter, evolution of the uniaxially oriented rod-like domains always results in the formation of coarser microstructure than that in the isotropic case. This indicates, for example, that a uniaxially stretching load on the system will result in faster directional coarsening of the microstructure.

Fig. 2 shows the snapshot pictures at several times for (a–d) a system of $C_0 = 0.50$, $J = 0.60k_BT$ and

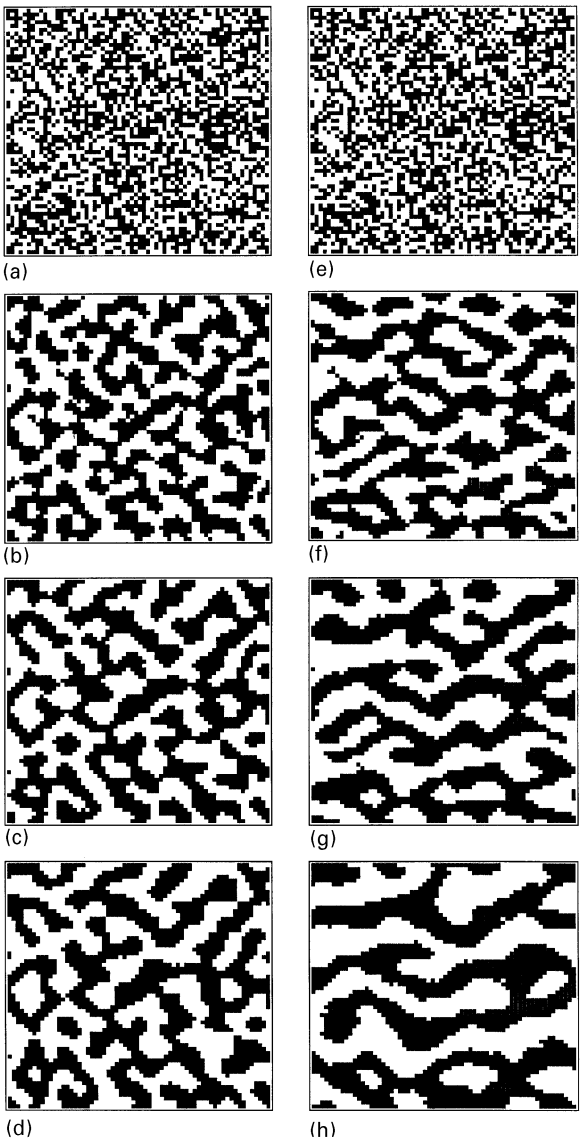

Figure 2 The snapshot pictures of the domained structure at several times for the systems (a–d) $C_0 = 0.50$, $J = 0.60k_BT$ and $\sigma = 0$ and (e–h) $C_0 = 0.50$, $J = 0.60k_BT$ and $\sigma = 0.50k_BT$. The solid spots are for B-type species and the open spaces for A-type species. The time scales are: (a) $t = 0$, (b) $t = 100$ mcs, (c) $t = 1100$ mcs, (d) $t = 3800$ mcs, (e) $t = 0$, (f) $t = 100$ mcs, (g) $t = 900$ mcs, (h) $t = 3900$ mcs.

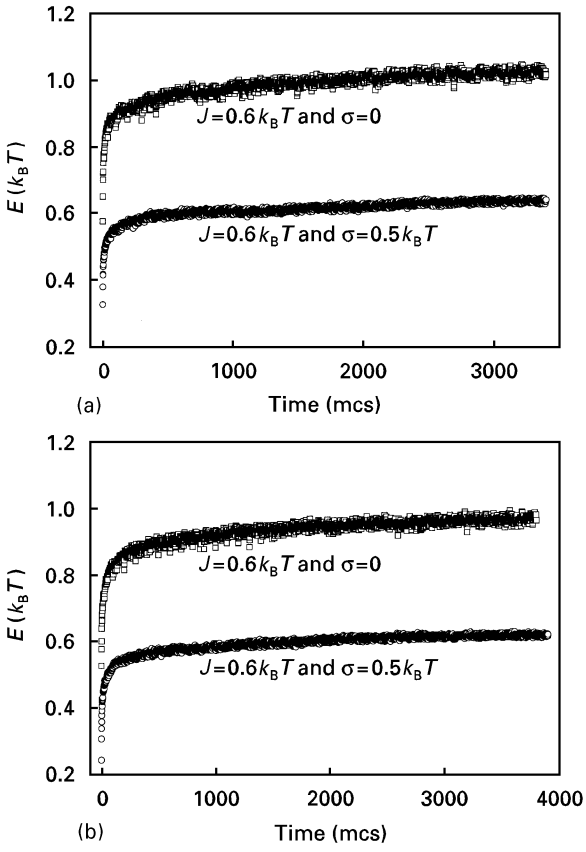

Figure 3 The averaged binding energy for each species in the lattices as a function of time. (a) $C_0 = 0.30$ and (b) $C_0 = 0.50$. The values of J and σ are given.

$\sigma = 0$ and (e–h) a system of $C_0 = 0.50$, $J = 0.60k_BT$ and $\sigma = 0.50k_BT$. Although both systems achieve inter-connected domained structure during phase separation, the morphology of the second-phase domains in the uniaxially anisotropic system ($\sigma = 0.50k_BT$) is stripe-like along the X-axis. The uniaxial stripes are quite wavy and become increasingly coarser by a process where the neighbouring stripes first touch and then join, reducing the number of stripes in the system. The kinetics of coarsening for the case of $\sigma = 0.50k_BT$ is much faster than the case of $\sigma = 0$, similar to the case shown in Fig. 1.

Fig. 3 gives the averaged binding energy, E, for each species in the lattice as a function of time, for several systems. In the very beginning stage, E shows a rapid growth and then slows down considerably. The time dependence of E in the later stage can be fitted with a power function. For all systems shown in Fig. 3, the exponent has been found to be 0.04. As pointed out earlier, E for the cases of $\sigma = 0.50k_BT$ is lower than that for the cases of $\sigma = 0$, but a coarser-domained structure forms in the former cases. Our simulations also show that with increasing σ, the uniaxially anisotropy of the domained structure also increases.

3.2. Correlation functions

Currently, the domain morphology and dynamics of phase separation can be quantitatively characterized by the spatial correlation function. The size, distribution and anisotropy of the domained structure can be estimated from the correlation function analysis. As a function of the lattice distance $R(t)$ which starts from zero, the correlation function shows oscillation around zero. The first zero point, $R(t) = R_1(t)$, scales the domain size and the second zero point, $R(t) = R_2(t)$, scales the domain spacing (i.e. modulating periodicity). Here, we only look at the uniaxial and radially averaged correlation functions $g(x)$, $g(y)$ and $g(r)$. The first zero points for these functions are denoted by $R_x(t)$, $R_y(t)$ and $R_r(t)$, respectively.

Figs 4 and 5 present, respectively, the water-fall plots of the uniaxial function $g(x)$ with time, for the isotropic systems ($\sigma = 0$) and the uniaxially anisotropic systems ($\sigma = 0.50k_BT$). As $\sigma = 0$ (Fig. 4a where

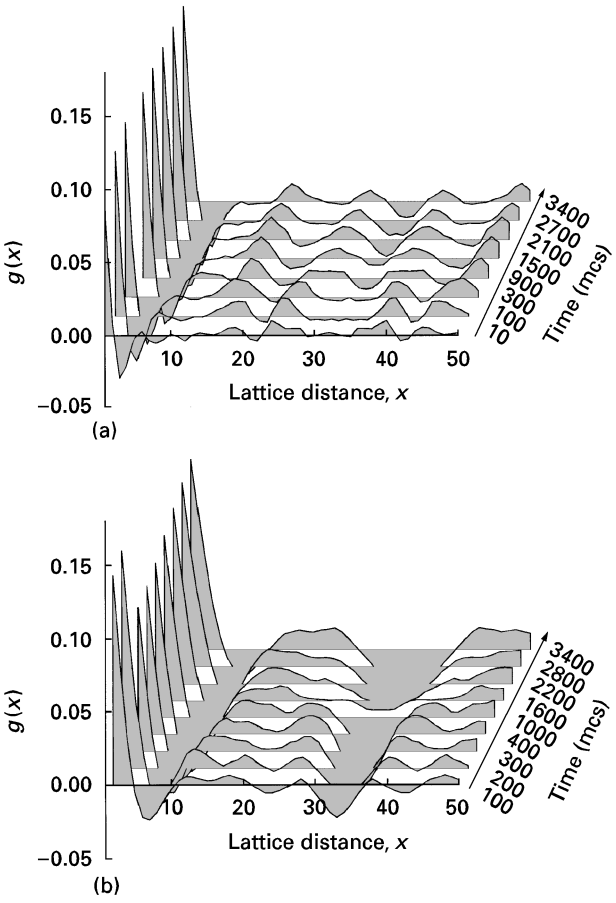

Figure 4 The water-fall plots showing the X-axially oriented spatial correlation function $g(x)$ against the lattice distance x at different times, for the systems (a) $C_0 = 0.30$, $J = 0.60k_BT$ and $\sigma = 0$ and (b) $C_0 = 0.30$, $J = 0.60k_BT$ and $\sigma = 0.50k_BT$. The arrows indicate the time flow.

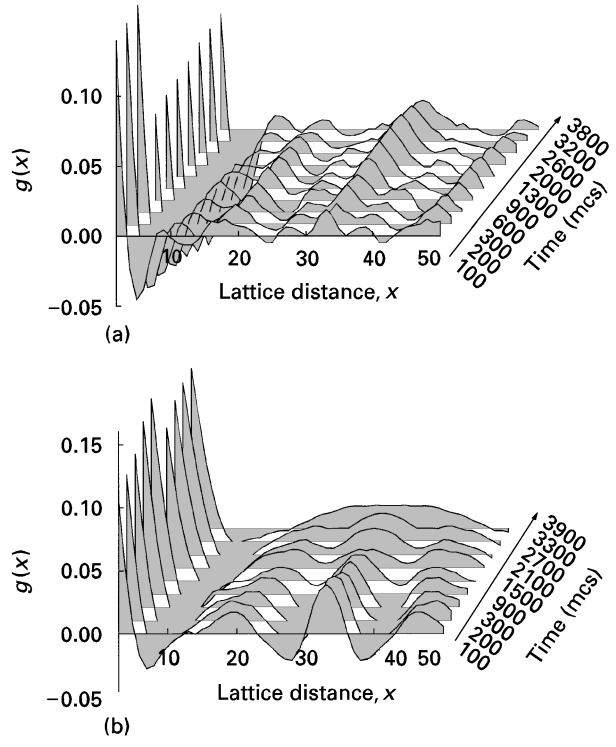

Figure 5 The water-fall plots showing the X-axially oriented spatial correlation function $g(x)$ against the lattice distance x at different times, for the systems (a) $C_0 = 0.50$, $J = 0.60k_BT$ and $\sigma = 0$ and (b) $C_0 = 0.50$, $J = 0.60k_BT$ and $\sigma = 0.50k_BT$. The arrows indicate the time flow.

$C_0 = 0.30$ and Fig. 5a where $C_0 = 0.50$), $g(y)$ and $g(r)$ show similar patterns as $g(x)$ and so we look only at $g(x)$. At any fixed time, against the lattice distance x, $g(x)$ decreases rapidly from a positive value and passes through $g(x) = 0$, and then starts oscillating. With time, R grows gradually, indicating coarsening of the domained structure. The oscillation pattern of $g(x)$ with x is relatively irregular at the early stage and evolves into relatively regular and roughly periodic ones, by a process whereby some peaks and valleys gradually decay and finally disappear, revealing that the distribution of the two-domained phases becomes more and more uniform. However, as the uniaxial anisotropy is involved, the evolution of the correlation function $g(x)$ (Fig. 4b where $C_0 = 0.30$ and Fig. 5b where $C_0 = 0.50$) becomes much faster than $g(y)$ and the symmetry is broken, demonstrating directional coarsening and indicating the formation of uniaxially anisotropic domained structure. Growth of R_x is also much more rapid than that of R_y. No periodic oscillation of $g(x)$ for the system of $C_0 = 0.50$ and $\sigma = 0.50k_BT$ can be identified here, because no structure modulation is induced along the X-axis as the periodic boundary conditions are applied.

3.3. Structure function

The structure function of the phase-separating system represents the spatial correlation of composition in the scattering geometry. The two-dimensional profiles and equal-height contours of $S(k_x, k_y)$ at $t = 3400$ mcs for the system of $C_0 = 0.30$ and $\sigma = 0$, and the system of $C_0 = 0.30$ and $\sigma = 0.50k_BT$, are given in Fig. 6a and b, respectively. For the case of $\sigma = 0$, clearly the structure function is roughly isotropic in the wave-vector space, and as a function of any wave-vector $\boldsymbol{k} = \boldsymbol{i}k_x + \boldsymbol{j}k_y$ which passes through $\boldsymbol{k} = 0$, the structure function shows a similar pattern of symmetric double-peaks around $\boldsymbol{k} = 0$. This is in agreement with those results presented earlier. However, for the case of $\sigma = 0.50k_BT$, the two-dimensional profile of $S(k_x, k_y)$ exhibits two sharp peaks along the line of $\boldsymbol{k} = \boldsymbol{j}k_y$, whereas the peaks along $\boldsymbol{k} = \boldsymbol{i}k_x$ are quite weak, as shown in the equal-height contour. This is a typical profile of the structure function for a system exhibiting strongly textured structure along the X-axis, as shown in Fig. 1, demonstrating again that directional coarsening proceeds in the domained structure. The double peaks along $\boldsymbol{k} = \boldsymbol{j}k_y$ for the case of $\sigma = 0.50k_BT$ are much higher and sharper than those displayed in Fig. 6a, indicating that the Y-axially oriented structure modulation in the case of $\sigma = 0.50k_BT$ is more perfect than arbitrarily oriented structure modulation in the case of $\sigma = 0$.

For the systems of $C_0 = 0.50$ and $\sigma = 0$, and $C_0 = 0.50$ and $\sigma = 0.50k_BT$, the two-dimensional profiles and equal-height contours of the structure function at $t = 3400$ mcs are shown in Fig. 7a and b, respectively. Similar characteristics to those shown in Fig. 6 are revealed. The peaked pattern of $S(k_x, k_y)$ along $\boldsymbol{k} = \boldsymbol{i}k_x$ is too hard to identify, owing to the

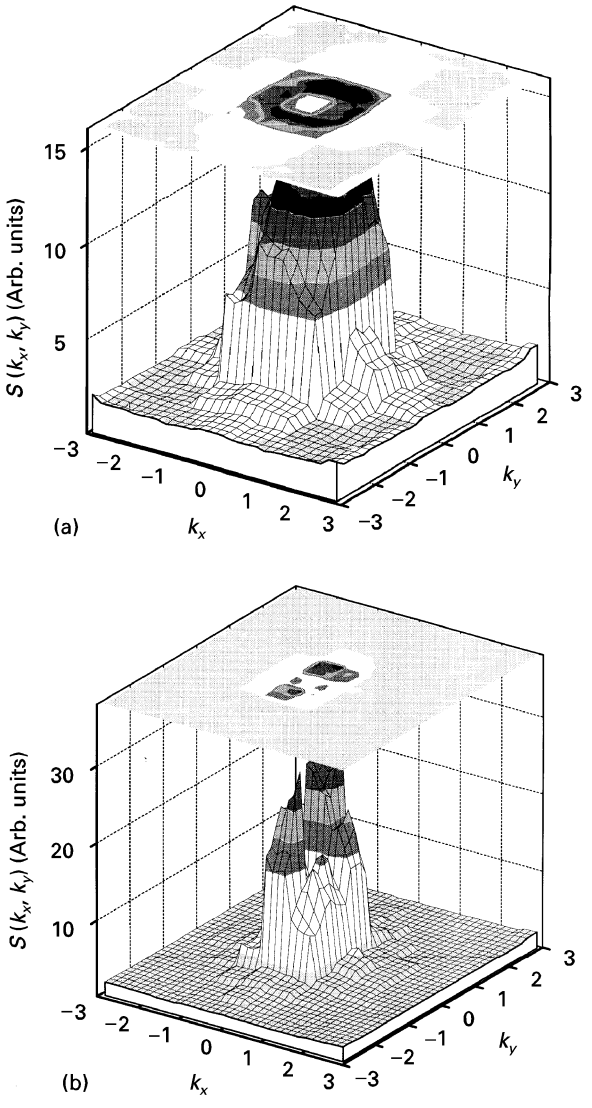

Figure 6 The two-dimensional profiles and equal-height contours of the structure function at $t = 3400$ mcs, for the systems (a) $C_0 = 0.30$, $J = 0.60k_BT$ and $\sigma = 0$ and (b) $C_0 = 0.30$, $J = 0.60k_BT$ and $\sigma = 0.50k_BT$.

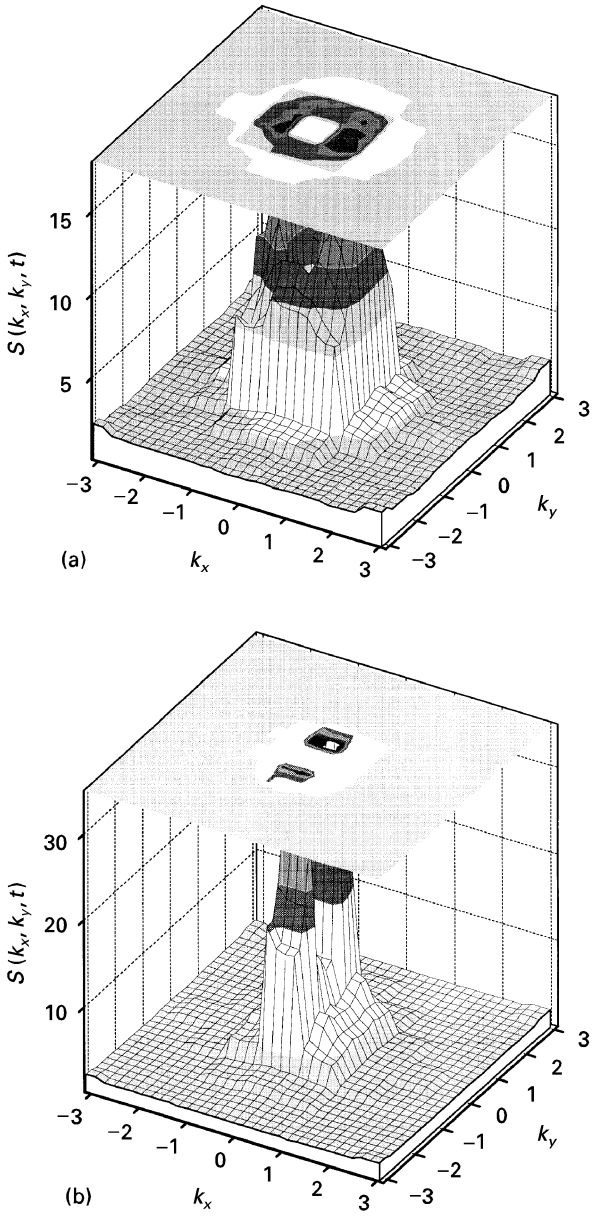

Figure 7 The two-dimensional profiles and equal-height contours of the structure function at $t = 3400$ mcs, for the systems (a) $C_0 = 0.50$, $J = 0.60k_BT$ and $\sigma = 0$ and (b) $C_0 = 0.50$, $J = 0.60k_BT$ and $\sigma = 0.50k_BT$.

fact that here no structure modulation occurs because of the applied periodic boundary conditions. The two peaks shown in Fig. 7b are much sharper than those shown in Fig. 6b, owing to more perfect structure modulation along the Y-axis for the former case.

3.4. Dynamic scaling

A dynamic scaling state means that all structural properties of the phase-separating system which are rescaled by the characteristic length of the domained structure, hold stationary with time except the characteristic length itself. This is a crucial property for the first-order transitions and has been verified in many isotropic systems ($\sigma = 0$). Because here we are dealing with the uniaxially anisotropic system, the dynamic scaling should be orientation-dependent. Because of the conservation property of the order parameter, the scaling transforms for the correlation functions can be written [16]

$$\eta = \frac{R(t)}{R_1(t)} \begin{cases} g(x) \to g(\eta), & R(t) = x \text{ and } R_1(t) = R_x(t) \\ g(y) \to g(\eta), & R(t) = y \text{ and } R_1(t) = R_y(t) \\ g(r) \to g(\eta), & R(t) = r \text{ and } R_1(t) = R_r(t) \end{cases} \tag{6}$$

For the systems of $C_0 = 0.30$ and $C_0 = 0.50$, as $\sigma = 0.50k_BT$ the correlation functions at different times, rescaled by following Equation 6 are presented in Figs 8 and 9, respectively. As $C_0 = 0.30$, it is clearly shown that by scaling transformation, all data of $g(x)$, $g(y)$ and $g(r)$ after $t = 400$ mcs fall quite well on to the same curves $g(\eta)$, respectively, demonstrating that the dynamic scaling is followed by the directional coarsening. Similarly, for the case of $C_0 = 0.50$, after $t = 400$ mcs, the system also reaches the dynamic scaling state. Note here that the rescaled $g(x)$ at different

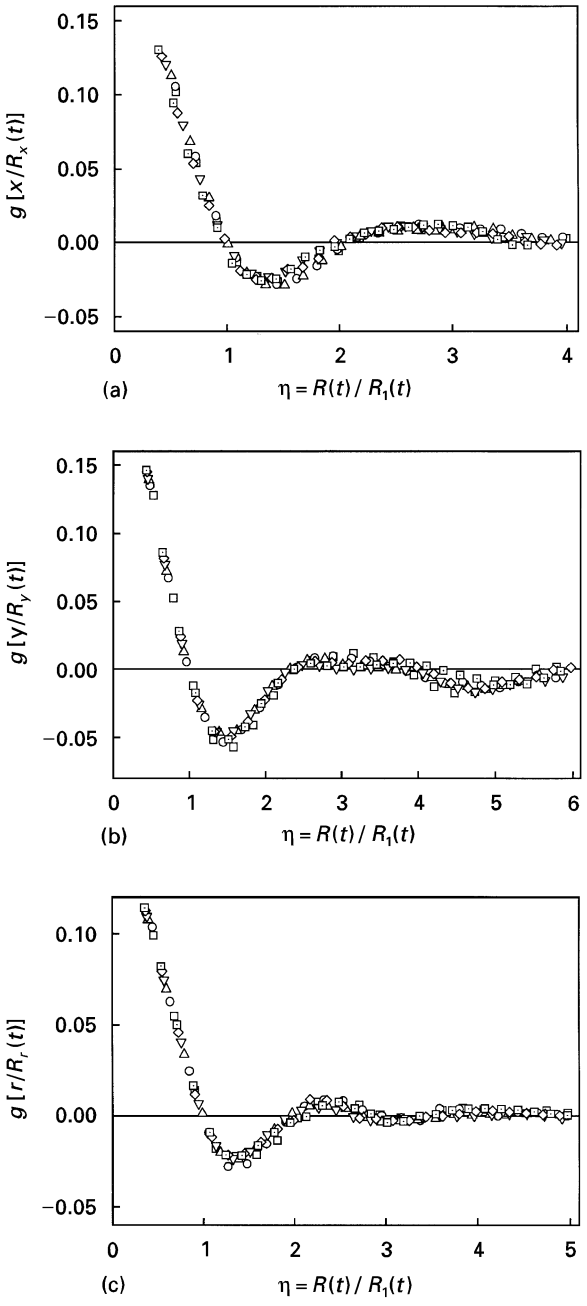

Figure 8 The spatial correlation functions (a) $g(x)$, (b) $g(y)$ and (c) $g(r)$ at several times, rescaled by the scaling transform $\eta = R(t)/R_1(t)$, for the system of $C_0 = 0.30$, $J = 0.60k_BT$ and $\sigma = 0.50k_BT$. The time scales are: (□) 400 mcs, (○) 1000 mcs, (△) 1600 mcs, (▽) 2200 mcs, (◇) 2800 mcs, (⊡) 3400 mcs.

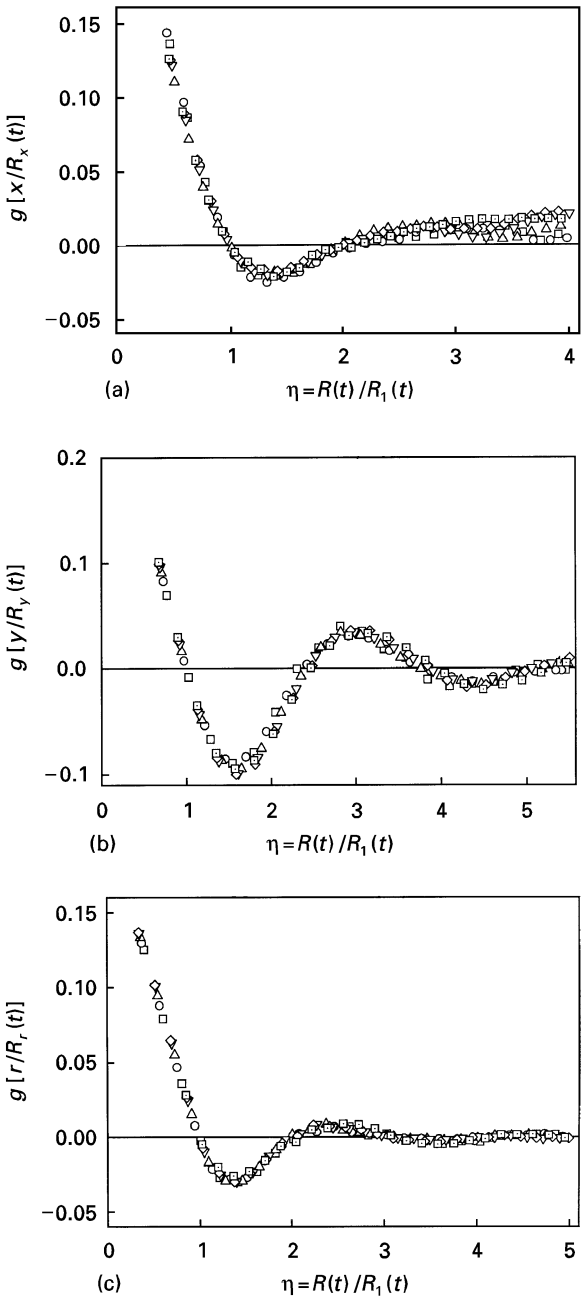

Figure 9 The spatial correlation functions (a) $g(x)$, (b) $g(y)$ and (c) $g(r)$ at several times, rescaled by the scaling transform $\eta = R(t)/R_1(t)$, for the system of $C_0 = 0.50$, $J = 0.60k_BT$ and $\sigma = 0.50k_BT$. The time scales are: (□) 900 mcs, (○) 1500 mcs, (△) 2100 mcs, (▽) 2700 mcs, (◇) 3300 mcs, (⊡) 3900 mcs.

times show worse consistency to each other as $\eta > 3$. This is obviously due to the statistical errors induced by the periodic boundary conditions. Therefore, we can conclude that towards the later stage, the directional coarsening in a uniaxially anisotropic system can acquire a dynamic scaling state.

3.5. Coarsening exponent

After demonstrating the dynamic scaling property, we return to examine another important property of the directional coarsening, i.e. the kinetic exponent of coarsening. Bearing in mind the uniaxial anisotropy of the domained structure, it is necessary to check separately the orientation-dependent exponents. These exponents are evaluated by plotting the axially oriented characteristic scales of the domained structure, R_x, R_y and R_r against time via a power function. The results are given in Fig. 10, where the spots represent the simulated data and the lines (solid, dashed and dot) are the best fits by the power function $R_1(t) \sim t^{1/3}$. For all cases, the simulated kinetics of coarsening follows quite well the Lifshitz–Slyozov–Wagner law [2]

$$R_1(t) = R_0 + at^{1/3}, \qquad R_0 > 0, \quad a > 0 \qquad (6)$$

Clearly, the early stage's deviations of the simulated data from the lines come from the constant term of Equation 7. From Fig. 10 we see that there always

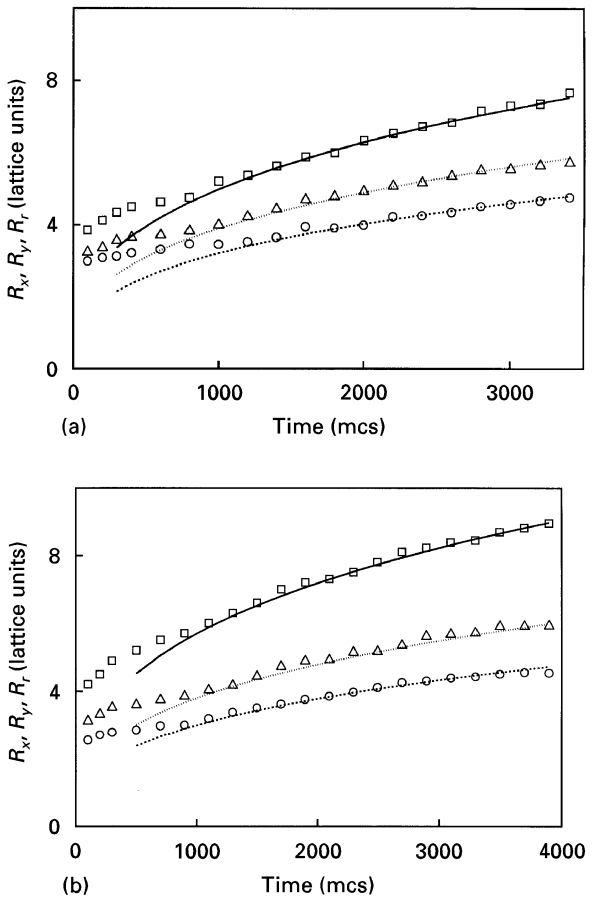

Figure 10 The axially oriented characteristic lengths (□) $R_x(t)$ and (○) $R_y(t)$, and (△) the radially averaged characteristic length $R_r(t)$, as functions of time, for the systems (a) $C_0 = 0.30$, $J = 0.60k_BT$ and $\sigma = 0.50k_BT$ and (b) $C_0 = 0.50$, $J = 0.60k_BT$ and $\sigma = 0.50k_BT$. Best fittings of (—) $R_x(t)$, (- - -) $R_y(t)$ and ($\cdots$) $R_r(t)$, following the 1/3 power function (see text), are shown.

exists $R_x(t) > R_r(t) > R_y(t)$ and towards the later stage, a constant ratio of $R_x(t)$ over $R_y(t)$ is achieved, indicating that the shape of domains may remain unchanged in the later stage. This is reasonable, when considering the dynamic scaling and Equation 7.

From all the results presented above, we may conclude that phase separation in a system of uniaxially anisotropic interaction does not exhibit fundamentally different dynamic properties from those for the isotropic system, although these properties are shown to be orientation-dependent.

4. Conclusion

The dynamics of directional coarsening in binary alloys with uniaxially anisotropic interaction has been studied by means of the Monte-Carlo technique. The time evolution of the morphology, the spatial correlation function and the structure function of the domained structure during phase separation have been presented in detail. It has been shown that because of the uniaxially anisotropic interaction, the system achieves uniaxial anisotropic morphology of domains and directional coarsening. The kinetics of coarsening is accelerated, compared to the isotropic system. The high pattern symmetry of the spatial correlation function and structure function of the domained structure are broken due to the directional coarsening. However, the dynamic scaling analysis reveals that towards the later stage, either the axially oriented correlations or their radial averages exhibit the dynamic scaling property, demonstrating the validity of the dynamic scaling hypothesis in approaching the dynamics of directional coarsening. A kinetic exponent of 1/3 for the directionally coarsened domain structure, independent of the orientation, is achieved, agreeing with prediction of the Lifshitz–Slyozov–Wagner theory.

Acknowledgements

The author thanks the Alexander von Humboldt Foundation of Germany for the financial support of this work. The hospitality of the Hahn-Meitner-Institut Berlin of Germany where the simulation was carried out is gratefully acknowledged.

References

1. J. D. GUNTON, M. SAN MIGUEL and P. S. SAHNI, in "Phase Transitions and Critical Phenomena", Vol. 8, edited by C. Domb and J. L. Lebowitz (Academic Press, New York, 1983) p. 267.
2. R. WAGNER and R. KAMPMANN, in "Materials Science and Technology: A Comprehensive Treatment", Vol. 5, edited by R. W. Cahn, P. Haasen and E. J. Kramer (VCH, New York, 1991) p. 213.
3. K. BINDER, *ibid.* p. 405.
4. P. HAASEN, V. GEROLD, R. WAGNER and M. F. ASHBY (eds), "Decomposition of Alloys: The Early Stages" (Pergamon Press, London, 1984).
5. A. G. KHACHATURYAN, "Theory of Structural Transformations in Solids" (Wiley, New York, 1983).
6. K. BINDER, in "Advances on Phase Transitions and Disorder Phenomena", edited by G. Busiello, L. De Cesare, F. Mancini and M. Marinaro (World Scientific, Singapore, 1987) p. 1.
7. A. CRAIEVICH and J. M. SANCHEZ, *Phys. Rev. Lett.* **18** (1981) 1308.
8. H. FURUKAWA, *Adv. Phys.* **34** (1985) 703.
9. K. BINDER and D. W. HEERMANN, in "Scaling Phenomena in Disordered Systems", edited by R. Pynn and A. Skjeltorp (Plenum Press, New York, 1985) p. 207.
10. H. FURUKAWA, in "Dynamics of Ordering Processes in Condensed Matter", edited by S. Komura and H. Furukawa (Plenum Press, New York, 1988) p. 35.
11. J. A. MARQUSEE and J. ROSS, *J. Chem. Phys.* **79** (1983) 373.
12. P. W. VOORHEES, *J. Stat. Phys.* **38** (1985) 231.
13. D. A. HUSE, *Phys. Rev. B.* **34** (1986) 7845.
14. J. G. AMAR, F. E. SULLIVAN and R. D. MOUNTAIN, *ibid.* **37** (1988) 196.
15. S. W. KOCH, R. C. DESAI and F. F. ABRAHAM, *Phys. Rev. A* **27** (1983) 2152.
16. T. M. ROGERS, K. R. ELDER and R. C. DESAI, *Phys. Rev. B* **37** (1988) 9638.
17. J. J. HOYT and D. DE FONTAINE, *Acta Metall.* **37** (1989) 1611.
18. S. POLAT, H. CHEN and J. E. EPPERSON, *Metall. Trans.* **20A** (1989) 1611.
19. J. MARRO, J. L. LEBOWITZ and .M. H. KALOS, *Phys. Rev. Lett.* **4** (1979) 282.
20. J. L. LEBOWITZ, J. MARRO and M. H. KALOS, *Acta Metall.* **30** (1982) 297.
21. J. D. ESHELBY, *Prog. Solid Mech.* **2** (1961) 89.
22. J. W. CAHN, *Acta Metall.* **10** (1962) 179.
23. H. NISHIMORI and A. ONUKI, *Phys. Rev. B* **42** (1990) 980.

24. T. MIYAZAKI and M. DOI, *Mater. Sci. Engng A* **110** (1989) 175.
25. F. LANGMAYR, P. FRATZL, G. VOGL and M. MIEKELEY, *Phys. Rev. B* **49** (1994) 759.
26. C. A. LABERGE, P. FRATZL and J. L. LEBOWITZ, *Phys. Rev. Lett.* **75** (1995) 4448.
27. J. K. TIEN and S. M. COPLEY, *Metall. Trans.* **2** (1971) 215.
28. J. C. CHANG and S. M. ALLEN, *J. Mater. Res.* **6** (1991) 1843.
29. S. SOCRATE and D. M. PARKS, *Acta Metall. Mater.* **41** (1993) 2185.
30. P. FRATZL and O. PENROSE, *ibid.* **43** (1995) 2921.
31. J. M. LIU, *J. Mater. Sci. Lett.* **14** (1995) 1734.

Received 16 February
and accepted 17 September 1996